Controlled Drift: An Investigation into the Controllability of Underwater Vehicles with Minimal Actuation

Ryan N. Smith[†] **and Matthew Dunbabin**[‡]
[†]School of Engineering Systems, Queensland University of Technology, Brisbane, QLD 4000, Australia.
[‡]Autonomous Systems Laboratory, CSIRO ICT Centre, P.O. Box 883, Kenmore, QLD 4069, Australia.
ryan.smith@qut.edu.au, matthew.dunbabin@csiro.au

Abstract

This paper is directed towards providing an answer to the question, *Can you control the motion of a Lagrangian float?* By design, a float has minimal actuation (only buoyancy control), and their horizontal motion is dictated by ocean currents (Lagrangian). With the appropriate vertical actuation, and utilising spatiotemporal variations in water speed and direction, we show here that broad controllability results can be met, such as waypoint following to keep a float inside or outside of a designated region. This paper extends experimentally validated techniques for utilising ocean current models to control horizontally actuated autonomous underwater vehicles by presenting an initial investigation into the application of these methods on minimally-actuated drifting floats. Simulated results for an offshore coastal region and a region within a highly dynamic tidal bay illustrates two scenarios promising an affirmative answer to the initially posed question.

1 Introduction

In the area of control theory applied to mechanical systems, it is interesting to consider systems that are underactuated, subjected to external forcing or have unique methods of actuation and locomotion. Examples of such research can be seen across a wide variety of disciplines, however the intersection of these three interesting control problems realizes itself in practical applications for the control of underwater vehicles. For example, such systems can be underactuated (e.g., torpedo-shaped vehicles [Hydroid, LLC, 2008]), subjected to external forcing (i.e., ocean currents), and have unique methods of propulsion (e.g., biomimetic [Morgansen *et al.*, 2007], energy harvesting [Manley and Wilcox, 2010] and variable buoyancy [Webb Research Corporation, 2008]). For these reasons, control theory for Autonomous Underwater Vehicles (AUVs) is a heavily studied area with many open questions, practical applications and interesting problems.

A key limitation for actively-actuated vehicles is their long-term endurance. The oceanographic community has a necessity for persistent observation platforms that remain *in situ* for months, and even years. Consequently, less actuated vehicles have emerged, resulting in energy savings and increased endurance – hence the rapid utilisation of ARGO profiling floats [Roemmich *et al.*, 2004]. With reduced actuation, these vehicles are less able to achieve reliable trajectories, as their motion is dictated more by external forces (ocean currents) than by their own power (thrusters). Hence, the primary region of operation is the deep ocean. There is an increasing interest to operate this type of platform in highly-dynamic coastal environments confined regions like bays to examine long-term variability and evolving features. In such environments, if left uncontrolled, these AUVs would run aground or travel away from the desired sensing location.

A body of literature exists on path planning for actuated AUV in the presence of water currents [Petres *et al.*, 2007; Alvarez *et al.*, 2004; Garau *et al.*, 2005]. These studies primarily relate to quasi steady-state ocean currents without consideration of vehicle actuation limits and often not identifying infeasible paths particularly in strong ocean currents. An alternate approach to minimum energy continuous path planning was proposed by [Kruger *et al.*, 2007]. Here the authors considered vehicle actuation limits using a multi-dimensional cost function for generating energy and time optimum paths in estuarine environments. In an extension of this work a new optimal (time and energy) path planning approach was demonstrated with an actuated AUV in a highly dynamic embayment [Witt and Dunbabin, 2008]. This work illustrated the potential to use currents for improving vehicle range and endurance as well as waypoint control in regions with tidally varying obstacles.

In this paper, we consider the interesting question: *Can you control the trajectory of a Lagrangian float?* In particular, what if we were able to prescribe a mission or control strategy that allowed for these floats to be loosely controlled? Could we amass a few hundred floats off the

coast of South America with the intent to examine an El Niño event, or gather such floats to lie in the path of a tropical storm? Although we will see that it is non-trivial to control the vertical motion of a float, the question we pose is related to controlling the horizontal motion of the float. We will detail a precise definition of controllability and what assumptions we consider for the float in the sections to follow.

A Lagrangian float is considered an AUV, and presents many questions in the area of control. In particular, can we use some basic knowledge or predictive models of ocean currents and tides to, 1) keep a float on one side of a given line, 2) restrict a float to reside in one quadrant of the ocean, or 3) keep a float within a bounded region of the ocean? This work extends the theory and experimental campaigns conducted by the authors using ocean models to guide higher-actuated AUVs in the coastal ocean [Smith *et al.*, 2010] and in shallow embayments [Witt and Dunbabin, 2008].

2 Lagrangian Floats

Lagrangian floats are widely used to gather data throughout our world's oceans in a cost-effective manner. These data are used in part to help us understand (and eventually predict) changes in both the atmosphere and ocean resulting from short and long-term global climate change. Thousands of Lagrangian floats are deployed by ships of opportunity and sent off to gather data while drifting with the ocean's currents.

To be truly Lagrangian, a float should follow all three components of oceanic velocity on all time scales. However, effectively doing so requires a deep understanding about the factors that control float buoyancy and motion in a stratified and mixing ocean. Existing operational methods simply let the floats drift with ambient currents while performing a set vertical mission profile.

Throughout the history of oceanographic research, there have been many subsurface floats produced and implemented. The interested reader can find further details in [Rossby *et al.*, 1985; Davis, 1991; Davis *et al.*, 1992; D'Asaro *et al.*, 1996]. We consider a platform that has held a place in ocean science for multiple decades, and examine the potential to increase the autonomy and utilisation of such a vehicle. Next, we present three existing examples of Lagrangian floats that represent a range of their operational capabilities.

2.1 ARGO Floats

The origin of Argo floats goes back to the beginning of Lagrangian float development. These are the most prolific and least controllable float considered here. Currently, there are 3433 floats in operation (21 August, 2011), and more are being deployed all the time, see Fig. 1. The goal of the Argo project is to collect high-quality temperature and salinity profiles from the upper

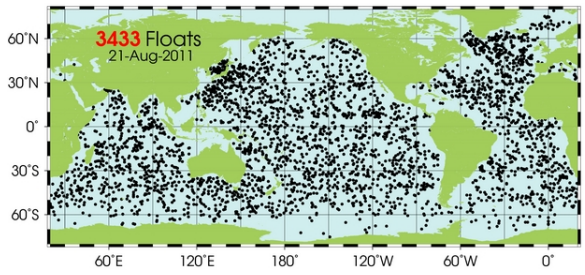

Figure 1: Current location of ARGO floats. Image courtesy of the Argo home page, `http://www.argo.ucsd.edu/index.html`.

2000 m of the ice-free global ocean, and currents from intermediate depths. At typically 10-day intervals, an Argo float surfaces over a 6-hour interval while measuring temperature and salinity. Satellites determine its position once on the surface and the collected data are transmitted. The float then returns to its original density and sinks to drift until the cycle is repeated. Currently, deployed floats are designed to make about 150 such cycles, which implies a deployment life of just over four years. There are two standard operating mission scenarios for Argo floats; the simple mission (see Fig. 2(a)), and the park and profile mission (see Fig. 2(b)).

2.2 SOLO-TREC Float

The Sounding Oceanographic Lagrangrian Observer (SOLO) Thermal RECharging (TREC), SOLO-TREC is a float that is completely powered by renewable energy; the temperature differences in the ocean. SOLO-TREC draws upon the ocean's thermal energy as it alternately encounters warm surface water and colder conditions at depth. This thermal engine produces about 1.7 watt-hours, or 6,100 joules, of energy per dive, enough electricity to operate the vehicle's science instruments, GPS receiver, communications device and buoyancy-control pump. SOLO-TREC has completed more than 300 dives from the ocean surface to a depth of 500 m and has demonstrated the capability of continuously executing $3-4$ dives per day.

2.3 University of Rhode Island Float

The University of Rhode Island (URI) Lagrangian float project is moving the basic Lagrangian float concept to shallow coastal waters, and developing a versatile and low-cost platform. These novel floats have an active ballasting system and acoustic altimeters, enabling them to position themselves anywhere in the water column, providing the ability to perform a range of drifting and profiling behaviours. Contrary to traditional deep water and upper ocean floats the URI floats are able to operate successfully in areas of highly-varied bathymetry, especially in near-shore environments.

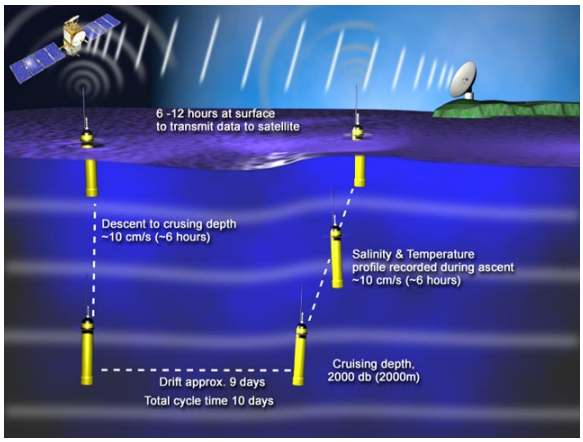

(a) Simple mission operation.

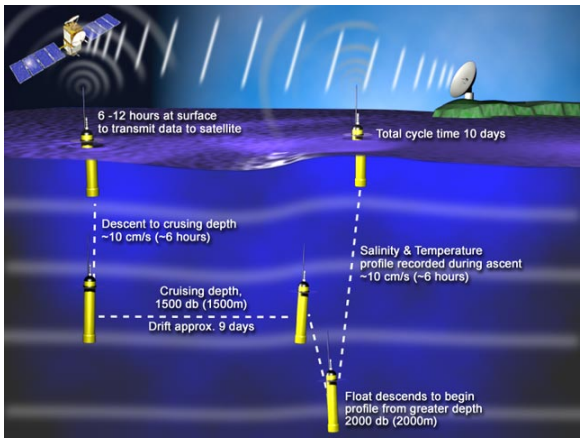

(b) Park and profile mission operation.

Figure 2: Standard missions executed by Argo floats. Images courtesy of the Argo home page, `http://www.argo.ucsd.edu/index.html`.

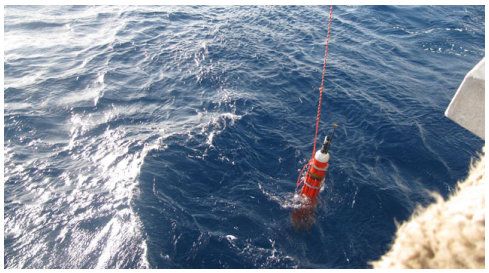

(a) The SOLO-TREC autonomous underwater vehicle is deployed off the coast of Hawaii on an ocean endurance test, Nov. 30, 2009. Credit: NASA/JPL/U.S. Navy/Scripps Institution of Oceanography.

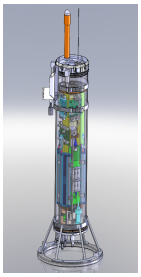

(b) A diagram of the URI Float.

Figure 3: Two additional types of Lagrangian floats.

With this additional controllability, the mission duration reduces to the order of days to weeks, as compared with the multi-year deployments of Argo and SOLO-TREC. Given the shallow depth rating and operating environment, this float avoids the complication of compressibility matching with either the pressure case design or compressible members that have been used many of the successful aforementioned isopycnal floats. The float is built around a piston-style, volume-changing mechanism allowing the buoyancy actuator to achieve profiling speeds of up to 20 m/min, with settling times O(10 s). For further information, see [Schwithal and Roman, 2009; McGilvray and Roman, 2010].

2.4 Assumed Float Characteristics

The characteristics of a float vary widely depending on the desired application. For the analysis presented here, we assume a system akin to that described in Section 2.3. We assume that the vertical position of the float within the water column can be controlled, albeit limited, and the horizontal velocity is determined strictly by ocean currents; varying with depth and geographic location.

3 Controllability

Consider a submerged rigid body that is stable in pitch and roll, and that is invariant to yaw orientation. In particular, we only consider actuation in surge, sway and heave, x, y, and z, respectively. We can express the equations of motion of this system, using the architecture of differential geometry [Bullo and Lewis, 2005], as a control-affine system $\Sigma = (Q, \mathcal{I} = \{\mathbb{I}_0, \mathbb{I}_1, ..., \mathbb{I}_m\}, U)$, where $Q = \mathbb{R}^3 \in \mathcal{C}^\infty$ is the configuration manifold (state space), $\mathcal{I}$ are $\mathcal{C}^\infty$ vector fields on Q, and the controls are given by $U \subset \mathbb{R}^m$. Thus, the differential equations representing the system state can be written as

$$\gamma'(t) = \mathbb{I}_0(\gamma(t)) + \Sigma_{a=1}^{m} u^a(t)\mathbb{I}_a(\gamma(t)), \qquad (1)$$

where $u : I \mapsto U \subset \mathbb{R}^m$ are the controls or inputs that take values in the set U. We assume the controls to be locally integrable, and when given, imply the existence of the locally absolutely continuous trajectory $\gamma : I \mapsto Q$ that takes values in the state manifold Q. The vector field $\mathbb{I}_0$ is commonly referred to as the *drift vector field*, and gives the dynamics of the system in the absence of user-defined control inputs. We refer to $\{\mathbb{I}_1, ..., \mathbb{I}_m\}$ as the input control vector fields for the system. In the case of the Lagrangian float system that we consider, the system can be defined on $Q = \mathbb{R}^3$ by

$$\dot{x_1} = f(t), \quad \dot{x_2} = g(t), \quad \dot{x_3} = u^3(t) + h(t), \qquad (2)$$

where $f(t), g(t)$ and $h(t)$ represent the horizontal (x, y) and vertical components of the ocean velocity, respectively, and $\{x_1, x_2, x_3\}$ define a right-hand, inertial coordinate system with x_3 chosen positive in the direc-

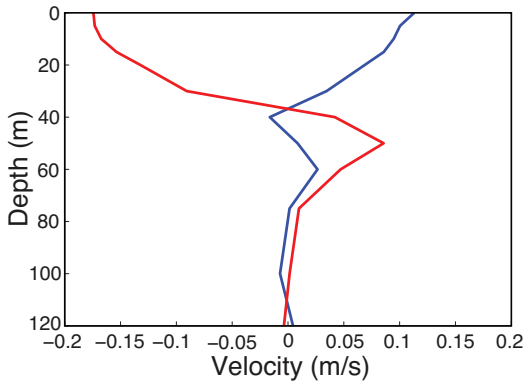

Figure 4: An example vertical current profile prediction for a location off the coast of southern California, USA. This is a ROMS prediction of ocean depth versus current velocity for the zonal (blue) and meridional (red) components located at 33.5° N, −118° E.

tion of gravity. By way of a simplification, we will initially ignore vertical currents, i.e., $h(z,t) = 0$, and thus $\dot{x_3} = u^3(t)$.

Note that we only have direct control on heave, i.e., the only input control vector field is $\mathbb{I}_1 = (0,0,1)^t$. For normal operation, the horizontal motion of the float is determined by the drift vector field $\mathbb{I}_0 = (f(t), g(t), 0)^t$, which is assumed to be solely determined by ocean currents. The existence of $\mathbb{I}_0$ in the state equations makes this a *forced* system, and with direct control only upon one degree-of-freedom, which is not along the axis of the external disturbances, one would initially consider this system uncontrollable. However, there is another way to formulate this same problem.

It is known that ocean currents are not constant functions with respect to depth, see Fig. 4. Thus, by varying the depth of the vehicle, we can indirectly control the horizontal motion. Hence, rather than include the ocean currents in the drift vector field $\mathbb{I}_0 = (f(t), g(t), 0)^t$, we can choose to write them as an input control vector field as functions of depth. Specifically, we define $\mathbb{I}_2 = H(z) = (f(z,t), g(z,t), 0)^t$, where $f, g : \mathbb{R}^+ \mapsto \mathbb{R}$ represent the zonal and meridional currents, respectively. Here, meridional velocity is positive eastward and zonal velocity is positive northward. This system can then be represented as a first-order, control-affine system on $Q = \mathbb{R}^3$ as

$$\gamma'(t) = \mathbb{I}_1 u^3(t) + \mathbb{I}_2 = \mathbb{I}_1 z(t) + \mathbb{I}_2. \tag{3}$$

Note here that we only include a control function $u^a(t)$ for the input vector field $\mathbb{I}_1$, as that is the only vector field that we can directly control. Since $\mathbb{I}_2$ is a function of depth and time, we obtain indirect control on this input vector field as we control the depth over time.

The reason for eliminating the drift vector field in the control-affine system given in Eq. (1) is to deal with a *driftless system*, for which standard controllability results are well-known and solutions calculated directly. We direct the reader to [Bullo and Lewis, 2005] for details on the differences between systems with and without drift vector fields. The primary reason for considering a driftless system is to avoid making the assumption that $f_0(x_0) = 0_{x_0}$, i.e., $f_0(x_0)$ is the zero vector in the fiber V_{x_0} of the associated vector bundle, to guarantee the controllability results given in [Sussmann, 1978]. Also, it is not practical to assume that the ocean current will be 0 in a given location x_0. Another reason for this approach is that instead of an unknown and uncontrolled drift on the system, we can use predictions from ocean models for the current velocities at given depths, giving us a way to estimate the controllability of the posed system. See Section 4 for information on the ocean models considered in this research.

Controllability for Control-affine Systems

The approach to examining the controllability of the system presented here follows from Chow's Theorem [Chow, 1939], and the extension of this result presented in [Sussmann and Jurdjevic, 1972]. These will be used to prove basic results for accessibility of the system, which will then provide necessary and sufficient conditions for the controllability of the system. We reproduce the following definitions from [Bullo and Lewis, 2005].

Definition 3.1 *A* controlled trajectory *of Σ is a pair (γ, u), where $u : I \mapsto U$ is locally integrable and $\gamma : I \mapsto Q$ is the corresponding locally absolutely continuous curve satisfying Eq. 1. We denote the set of controlled trajectories for Σ defined on $[0,T]$ by $C_{traj}(\Sigma, T)$.*

Definition 3.2 *For x_0 in Q, the set of states that are* reachable *in time exactly T is denoted by $\mathcal{R}_\Sigma(x_0, T) = \{\gamma(t) | (\gamma, u) \in C_{traj}(\Sigma, T), \gamma(0) = x_0\}$. Also, the set of states that are reachable in time* at most *T is given by $\mathcal{R}_\Sigma(x_0, \leq T) = \cup_{t\in[0,T]} \mathcal{R}_\Sigma(x_0, t)$.*

Definition 3.3 (Notions of Controllability) *Let $\Sigma = (Q, \mathcal{I} = \{\mathbb{I}_0, \mathbb{I}_1, ..., \mathbb{I}_m\}, U)$ be a $\mathcal{C}^\infty$-control-affine system and let $x_0 \in Q$.*

1. *Σ is* accessible *from x_0 if there exists $T > 0$ such that $int(\mathcal{R}_\Sigma(x_0, \leq t)) \neq$ for $t \in]0, T]$.*
2. *Σ is* controllable *from x_0 if, for each $x \in Q$, there exists $T > 0$ and $(\gamma, u) \in C_{traj}(\Sigma, T)$ such that $\gamma(0) = x_0$ and $\gamma(T) = x$.*
3. *Σ is* small-time locally controllable (STLC) *from x_0 if there exists $T > 0$ such that $x_0 \in int(\mathcal{R}_\Sigma(x_0, \leq t))$ for each $t \in]0, T]$.*

Since we consider a driftless system, we can invoke a local version of Chow's Theorem to infer the controllability. In particular, we state the following Corollary to the more general result of [Bianchini and Stefani, 1993].

Corollary 1 (Controllability of driftless systems) *Let $\mathcal{F} = \{f_0, f_1 \dots f_m\}$ be $\mathcal{C}^\infty$-vector fields on Q with f_0 identically zero. The pair $(Q, \mathcal{F})$ is properly STLC from x_0 if $Lie^\infty(\mathcal{F})_{x_0} = T_{x_0}Q$.*

Here, $\text{Lie}^l(\mathcal{D})$ is the distribution generated by Lie brackets of degree l in vector fields taking values in $\mathcal{D}$. For $l = \infty$, $\text{Lie}^l(\mathcal{D})$ represents the involutive closure of $\mathcal{D}$. From this result, the choice to write the drift vector field as a *controlled* input vector field should be evident. Next, we derive necessary and sufficient conditions for controllability.

Conditions for Controllability

We are interested in verifying controllability for Eq. (3) in $\mathbb{R}^2$. This can be accomplished by examining the accessibility set; the set of all admissible motions from each configuration.

Lemma 1 *Given $p \in \mathbb{R}^3$, the accessibility set for the system in Eq. (3) is given by $\mathcal{A} = Lie^\infty(\mathcal{I})$ for $\mathcal{I} = \{\mathbb{I}_1^{-1}, \mathbb{I}_2^{-1}\}$.*

From this result, we have the the following corollary.

Corollary 2 *Since $\mathbb{I}_1^{-1} = (0, 0, 1)^t$, $\mathcal{A} = (f^{(n)}(z), g^{(n)}(z), 0)^t$ for $n \in \mathbb{Z}^+$.*

The controllability of $\mathcal{A}$ is assessed by use of the following proposition.

Proposition 1 *The system given in Eq. (3) is kinematically controllable in $\mathbb{R}^2$ if and only if the convex hull of the accessibility set $\mathcal{A}$ is compact and contains the origin.*

The proof of Proposition 1 is a standard result from control theory, and in the interest of space, we omit the details here. We refer the interested reader to [Bullo and Lewis, 2005] for a proof of this result. From Proposition 1, we infer the following properties on f and g.

Lemma 2 *If the set $\mathcal{A}$ satisfies Proposition 1 and $\mathbb{I}_2^{-1} = (f(z), g(z), 0)^t$, then f and g must satisfy the following properties:*

1. *$\exists \mathcal{Z} = \{z_1, ..., z_n\}$, $n \geq 4$ such that $f(z_i) \times g(z_i) \neq 0$, and*
2. *$\exists \{\hat{z_1}, \hat{z_2}, \hat{z_3}, \hat{z_4}\} \in \mathcal{Z}$ such that:*
   - *$f(\hat{z_1}) \in \mathbb{R}^+$ and $g(\hat{z_1}) \in \mathbb{R}^+$*
   - *$f(\hat{z_2}) \in \mathbb{R}^-$ and $g(\hat{z_2}) \in \mathbb{R}^+$*
   - *$f(\hat{z_3}) \in \mathbb{R}^-$ and $g(\hat{z_3}) \in \mathbb{R}^-$*
   - *$f(\hat{z_4}) \in \mathbb{R}^+$ and $g(\hat{z_4}) \in \mathbb{R}^-$*

   where the $\hat{\cdot}$ operator designates a possible reordering of the elements of $\mathcal{Z}$.

The proof of Lemma 2 lies in the fact that for the accessibility set $\mathcal{A}$ to contain the origin, we must have an admissible velocity in each of the four quadrants of $\mathbb{R}^2$. Else, a set $\mathcal{A}$ can be constructed such that the convex hull does not contain the origin. Additionally, we can extend the result on Lemma 2 by replacing f and g with $f^{(n)}$ and $g^{(n)}$, $n \in \mathbb{Z}^+$, respectively. This is easily seen by applying the result of Corollary 2.

Proposition 1 and Lemma 2 present an analytic analysis of the control of a Lagrangian float that can move vertically through the water column. In practice, we must consider restrictions to the vertical motion of the float, and verifying the above necessary and sufficient conditions for a given region of the ocean is essentially impossible. The ocean is too dynamic and complex to incorporate into such an analytic formality. However, we can utilise general trends and ocean models to assist in planning and control techniques, since we are not interested in precise trajectory tracking but a more general notion of *control*. Next, we present the ocean models considered for use in field deployments, leading into the application of the presented theory.

4 Ocean Models

Two different ocean models are considered in this paper for evaluation and implementation of the actuated drifter trajectory control; (1) the Regional Ocean Modeling System, and (2) the Receiving Water Quality Model.

4.1 Regional Ocean Modeling System

A predictive tool that can be utilized for general open ocean currents in the pacific basin is the Regional Ocean Model System (ROMS) - a split-explicit, free-surface, topography-following-coordinate oceanic model. ROMS is an open-source, ocean model that is widely accepted and supported throughout the oceanographic and modelling communities. The model solves the primitive equations using the Boussinesq and hydrostatic approximations in vertical sigma (i.e., topography following) and horizontal orthogonal curvilinear coordinates. ROMS uses innovative algorithms for advection, mixing, pressure gradient, vertical-mode coupling, time stepping, and parallel efficiency. Detailed information on ROMS can be found in [Shchepetkin and McWilliams, 1998] and [Shchepetkin and McWilliams, 2005]. Applications of this four-dimensional model implemented in AUV path planning can be found in [Smith *et al.*, 2010; 2011] and the references contained therein.

4.2 Receiving Water Quality Model

The Receiving Water Quality Model (RWQM) is a 2-D hydrodynamic and biogeochemical ocean forecast model using the RMA2 framework [King, 2004] developed for Moreton Bay in Queensland, Australia (see Figure 5(a)). The hydrodynamic simulation is provided using a non-uniform mesh with 8000 nodes that is driven by tidal boundary constraints and wind forecasts (Figure 5(b)). The original purpose for this simulation was focused on water quality management [Bell and Amghar, 2002]. The ocean simulation only solves currents in two spatial dimensions using an average of the currents in the

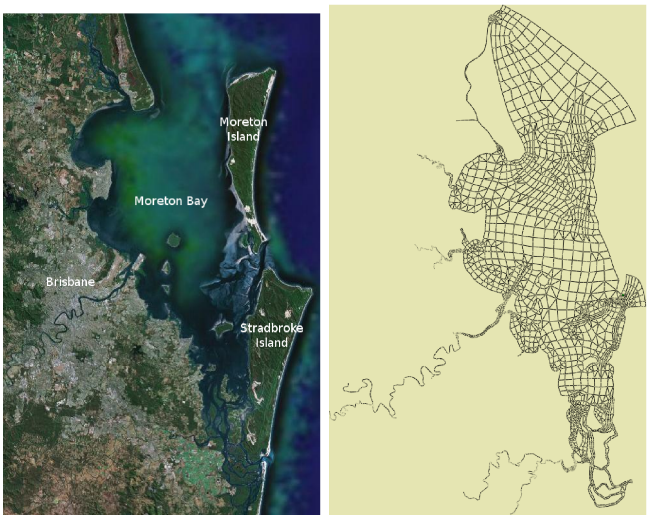

(a) (b)

Figure 5: (a) Moreton Bay near Brisbane in Australia (satellite image from Google Maps). (b) The non-uniform data grid of the current and bathymetry data with adaptive resolution (the corners and the mid-points of each line contain samples).

vertical direction. For use in Lagrangian float trajectory control considered here, the forecasts used in this paper have been extended to 3-D by approximating the vertical current distribution of boundary layer with a polynomial. Experimental validation for path planning using the RWQM was first presented in [Witt and Dunbabin, 2008]. Due to the topography with the two large islands, Moreton and Stradbroke Islands, and hundreds of smaller islands the currents are mostly driven by the tidal cycle. Thus the currents completely reverse direction within about six hours. Accordingly, a path taking 24 hours involves four current inversions along with time-variant obstacles due to tidal water level changes.

5 Controllability in the Coastal Ocean - ROMS

To initially assess the feasibility of controlling Lagrangian floats utilising data from predictive ocean models, we consider the criteria presented in Proposition 1 and Lemma 2 in Section 3 and an output from the ROMS. This model focuses on the coastal ocean region off the coast of southern California. The red dots in Fig. 6 represent the locations in the model satisfying Lemma 2 (top row) and Proposition 1 (bottom row) over a depth range of $0 - 125$ m. The columns in Fig. 6 represent the discrete time epochs $t = 0, 12$ and 24 hours.

In the images of Fig 6, we are interested in finding contiguous regions of controllability that remain over long periods of time, implying that a float would be able to remain within that area by changing its depth.

The locations guaranteeing controllability by satisfying the necessary condition presented in Lemma 2 are very sparse. In practice, this is a very strict condition on the relationship between f and g, as well as on the individual functions themselves. In particular, if $n(f)$ is the number of zeros of f, Lemma 2 imples that $n(f) \geq 1$, $n(g) \geq 1$, and $n(f) \geq n(g) + 1$ or $n(g) \geq n(f) + 1$. The later inequalities imply that the zeros of f and g are interlaced. Expecting ocean currents to posses specific properties over large regions is not practical, thus we consider the general result presented in Proposition 1.

The locations satisfying the controllability condition presented in Proposition 1 provide a more dense set than those of Lemma 2. This is because we are not guaranteeing specific properties of f and g, but simply ensuring that the origin is contained within the convex hull of the accessibility set. From the control theory laid out in Section 1, we can calculate the accessibility set at each node of a given ocean model. This provides a feasibility analysis of the given regions. The red dots in the bottom row of images in Fig. 6 represent locations where all directions of travel are feasible for a float. The large contiguous areas in Fig. 6 indicate that a float could remain within the presented region for at least 24 hours. Further analysis has shown this trend to exist for time scales on the order of weeks (seasonally dependent) for this region. These data provide motivation for seeking a control strategy that assigns a sequence of depth commands to a floating vehicle so that it follows a particular course, or remains within a given region.

6 Path Planning for a Lagrangian Float

In contrast to a general AUV, a Lagrangian float can only control its depth, and the resulting horizontal position is solely determined by the ambient currents. An important assumption for the path planning method presented here is that general ocean currents are not constant with respect to depth, see Fig. 4.

The vertical current in the 2-D ocean forecast model (Section 4.2) is modelled by a polynomial distribution that assumes small magnitude currents on the sea floor (bottom-boundary condition) and larger magnitude currents on the ocean surface (tidal and wind driven motion). Therefore, the distance travelled in a specific time step depends on the depth of the vehicle, as detailed in Section 3. It is assumed that the float can change its depth quickly compared to the duration of path execution. Thus, no constraint on changing depth between two adjacent nodes are imposed in this analysis.

Chassignet and Verron [Chassignet and Verron, 2006] provide an overview of drifting objects in the ocean. The velocity of a drifting object can be determined by $v_{drift} = v_{curr} + v_{rel}$, where v_{curr} is the velocity of the surrounding current and v_{rel} is the relative velocity caused by wind and waves. As long as the float away from

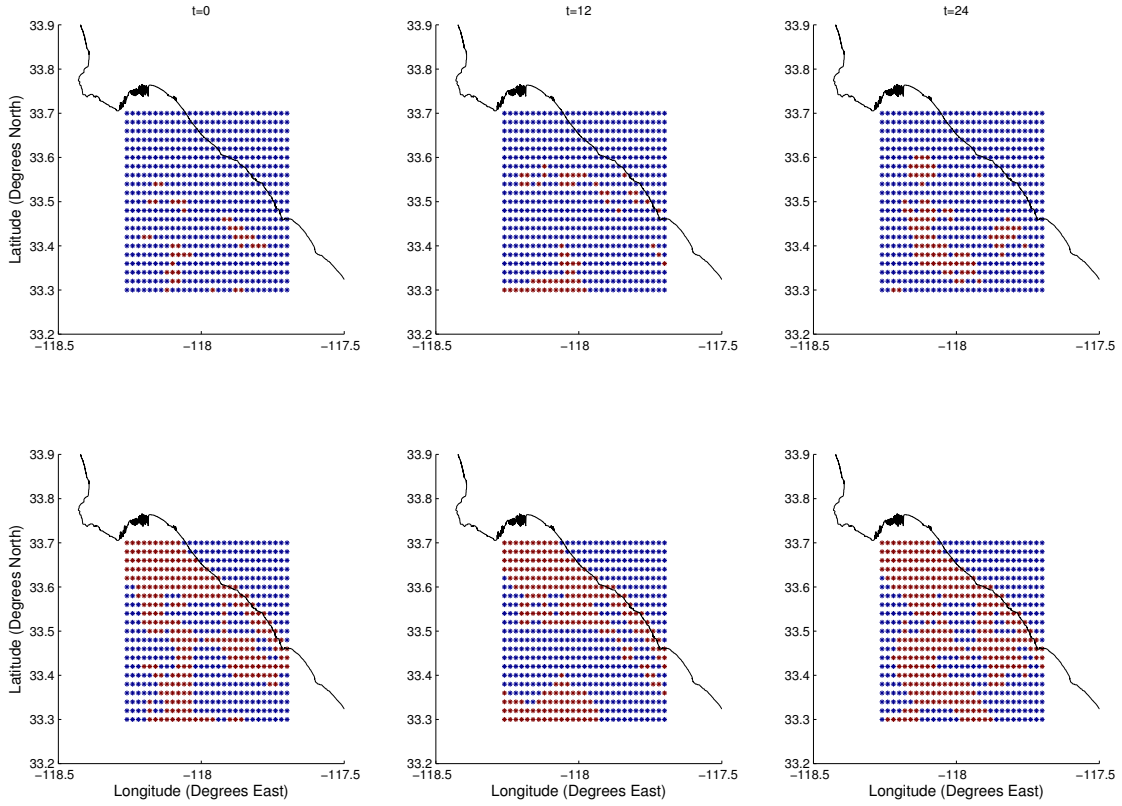

Figure 6: Locations in a region off the coast of southern California that satisfy Lemma 2 (red markers on the top row), and Proposition 1 (red markers on the bottom row) for a depth range of $0 - 125$ m. Time steps are $t = 0, 12$ and 24 hours.

the sea surface, there is negligible influence of wind and waves, therefore $v_{drift} = v_{curr}$. This is the assumption made in this study. Additionally, the period of acceleration to change the speed of the float can also be neglected [Chassignet and Verron, 2006]. This problem is fundamentally different from the path planning problem posed in [Witt and Dunbabin, 2008], as the accessibility set (reachable locations) of a Lagrangian float is highly limited.

Based on the limited controllability, we accept that the floats cannot reach every position, and it is not guaranteed that a float will precisely reach a goal location. In most cases, the floats only get to within a neighbourhood of the prescribed goal. In comparison to classical path planning, paths here are require several tidal periods to travel from start to goal.

6.1 Snapshot Technique

For the simulation, we utilise discretisation of the provided model for planning purposes. As the plans occur over multiple tidal cycles, and the floats travel relatively slowly, we need to correlate the appropriate time step into the control computation. This is especially critical in the presence of flood and ebb tides. In particular, when the tidal currents direct the float in the desired direction of travel, the drifter must be at the depth with strongest currents. During times of opposite tidal flow, the float must be at the depth with lowest magnitude currents.

To keep our algorithm simple and efficient, we implement a snapshot technique to identify the mean whole-of-bay tide extremes. This snapshot institutes a constant tidal period throughout the model. With this constant tidal period it is possible to use precomputed drifting paths between high and low tide. The current at each node is precomputed and stored in a separate model file. To be independent of absolute depth, the current at each of the nodes is simulated in three layers with different relative depths: 10%, 50% and 90%. The current at an arbitrary location is obtained by interpolating between the precomputed values. The horizontal direction (x, y), uses an inverse-distance weighting, and the vertical (z)

direction uses a polynomial interpolation.

Cost Function for Drifting

The general cost function used for our planning is given by Eq. (4). The most important measure in this cost function when considering a Lagrangian float is the distance to the prescribed goal location C_{dist}. Since the closest distance to the goal does not necessarily occur at the last node, the node with the closest distance to the goal must to be determined. The term C_{time} considers the time used to get to this closest position.

$$C_{total} = C_{dist} + w_t\, C_{time} + w_s\, C_{shallow} + w_e\, C_{energy} \quad (4)$$

Shallow water and the regions close to the surface can be incorporated in the cost function ($C_{shallow}$), but also can be eliminated by the optimisation algorithms when the depth is modified. A cost term for energy consumption C_{energy} can also be included in the cost function, but as changing the depth is necessary to control the vehicle, the influence must be low. In general, tuning the time weight has greater influence on the path length, and therefore on the energy consumption. Computing the energy cost is also difficult due to the shallow water. To stay in a specific depth, the buoyancy has to be controlled continuously.

Path Optimisation

The path optimisation is conducted in two steps. First, Simulated Annealing (SA) with precomputed drifts is used to determine a coarse path. Second, the path is refined by SA and a Local Random Search.

A single initial path at 50% depth is used to seed the path optimisation whereby the only parameter in the path that can be modified is the depth in each node. By use of relative depths, all parameters can be modified simultaneously, and the path is recomputed afterwards.

As the float can change depth quickly in comparison to the time step of the precomputed drifts, the path between two nodes is simulated as drifting at the same depth for the complete time step and then changing the depth in a step-wise fashion. When a coarse path with the precomputed drifts is found, the path is refined. Instead of using the precomputed drifts, each step is simulated with a smaller time step.

In the refinement step, deviations to the precomputed paths still occur. This can be improved by a local optimisation step. The new nodes are optimised to minimise the summed distance to the precomputed steps. After the refinement process, SA with a low initial temperature can be used again. For further optimisation, Local Random Search is used.

7 Results

To demonstrate the methods presented in the previous sections, we provide initial simulation results to analyse the feasibility of controlling a Lagrangian float in Moreton Bay, Queensland, Australia.

7.1 Trajectory Control in Shallow Bays - RWQM

A series of simulations were conducted to evaluate the feasibility of controlling the final destination of a vertically-actuated Lagrangian float in a shallow, highly dynamic environment; Moreton Bay. Using the methodology described in Section 6 and the extended ocean forecast model described in Section 4.2, a case study was devised whereby a float was commanded to move from one point of the bay to a southerly point over a period of 10 days, by use of only vertical (buoyancy) control.

Figure 7(a) shows an example simulation with no control applied to the float over a period of 10 days. As can be seen, the float follows the tidal cycling, and only moves in an easterly direction due to an underlying circulating current. After 10 days of drifting, the float made little progress towards the prescribed goal location. Figure 7(b) shows the resulting trajectory when the vertical position of the float is altered by use of the control strategy and optimisation presented in the previous sections. Here the path was terminated when the float reached a predefined distance from the goal location. The graph presented in Figure 7(c) shows a time history of the bathymetry (black line) and commanded float depth (blue line) of the controlled mission.

Through multiple simulations, the trajectory planner was found to reliably produce feasible paths with the limiting factor being the number of days the simulation was allowed to run. This allowed the results shown in Figure 7 to be extended to achieving multiple successive waypoints allowing gross trajectory control of drifters within Moreton Bay. It is hypothesised that application of the methods presented here would allow for a drifting AUV to remain within the bay for months at a time.

8 Conclusions

At the outset of this paper, we posed the question, *Can you control the motion of a Lagrangian float?* The presented study leads us to answer *Probably.*

We have provided a necessary condition on the functions defining ocean current with respect to depth for the controllability of a Lagrangian float. These strict conditions can be relaxed to the more general result presented in Proposition 1. We presented an analysis of the accessibility sets guaranteed by both Lemma 2 and Proposition 1. Data presented from Proposition 1 imply that broad controllability of a Lagrangian float is possible, under the assumption that the time required to change depth is negligible with respect to the duration of the proposed deployment time.

The control theory presented in Section 3 is validated via the simulation results presented in Section 7. In the presented results, we show that by simply controlling the operational depth of a float, we can guarantee broad controllability results, such as navigating from one loca-

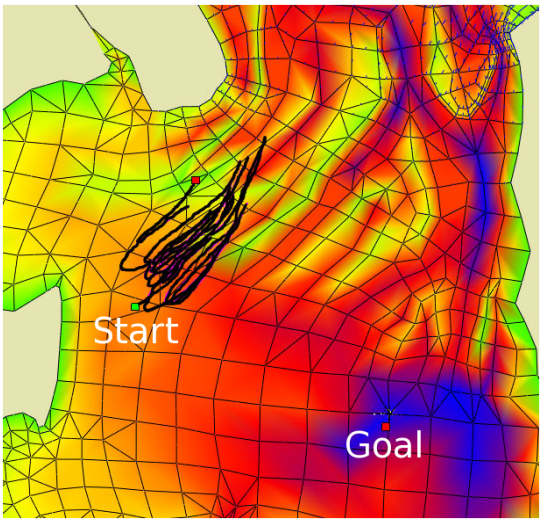

(a) The uncontrolled trajectory (black line) over a 10-day period.

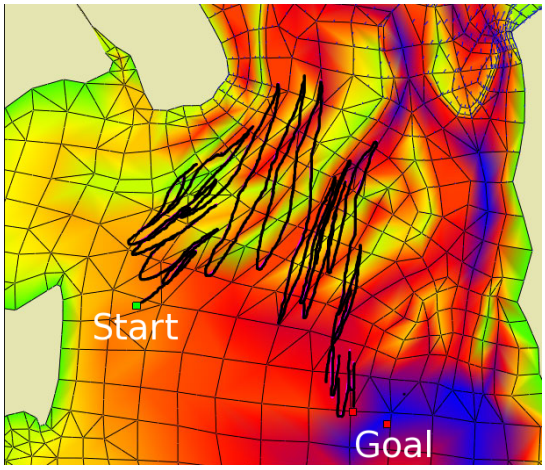

(b) The optimal depth-controlled trajectory (black line) from start to goal using predicted water currents over a 10-day period.

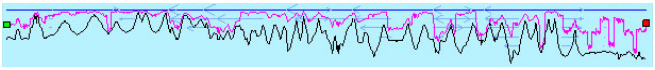

(c) The time history of bathymetry at the float location (black line) and commanded float depth (blue line)

Figure 7: Simulation of a drifter control experiment in Moreton Bay.

tion to another, or remaining within a given region for a long period of time. These results motivate field trials to further validate the control theory and path planning methods presented in this study.

8.1 Future Work

The results presented here hold as long as we allow the float to move vertically through the water column uninhibited; this is not actually the case. Thus, a model for the vertical motion of a float needs to be incorporated into the theory presented in Section 3 to provide a more precise prediction on the locations of controllability. Coupling this with a temporal analysis of the variability of the percentage of the region where a float can be controlled will provide valuable information for preparing for field deployments.

The simulation results presented in Section 7.1 provide ample motivation for performing field trials. For deployment of floats within shallow, coastal zones (depth less than 50 m), such as Moreton Bay, there will be a compromise between endurance and depth cycling capability. To this end, a new float system is currently under development. The aim is to design a vehicle that can exploit the controllability results presented here by moving vertically through the water column, and which has the ability to remain on deployment to capture the residence time of the bay ($\sim$ 3 months). This system would properly assess the validity of the hypothesis presented at the end of Section 7.1.

Acknowledgments

The authors would like to express their sincere thanks to Markus Schreiber for the simulation model refinement as well as Prof Tony Howes from the University of Queensland for supplying the Moreton Bay hydrodynamic forecasts. This work was supported in part by the Early Career Academic Recruitment and Development (ECARD) Program of the Queensland University of Technology. The ROMS ocean modeling research described in this publication was carried out by the Jet Propulsion Laboratory (JPL), California Institute of Technology, under a contract with the National Aeronautics and Space Administration (NASA).

References

[Alvarez *et al.*, 2004] Alberto Alvarez, Andrea Caiti, and Reiner Onken. Evolutionary path planning for autonomous underwater vehicles in a variable ocean. *IEEE Journal of Oceanic Engineering*, 29(2):418–429, 2004.

[Bell and Amghar, 2002] Simon Bell and Mohand Amghar. Modelling scenarios for south east queensland regional water quality management strategy. Technical report, Cooperative Research Centre for Coastal Zone, Estuary and Waterway Management, Queensland Government Environmental Protection Agency, February 2002.

[Bianchini and Stefani, 1993] R.M. Bianchini and G. Stefani. Controllability along a trajectory: A variational approach. *SIAM Journal on Control and Optimization*, 31(4):900–927, 1993.

[Bullo and Lewis, 2005] Francesco Bullo and Andrew D. Lewis. *Geometric Control of Mechanical Systems*. Springer, 2005.

[Chassignet and Verron, 2006] E.P. Chassignet and J. Verron, editors. *Ocean Weather Forecasting: An Integrated View of Oceanography*. Springer, 2006.

[Chow, 1939] W.-L. Chow. Über systemen von linearen partiellen differentialgleichungenerster ordnung. *Mathematische Annalen*, 117:98–105, 1939.

[D'Asaro *et al.*, 1996] Eric A. D'Asaro, David M. Farmer, James T. Osse, and Geoffrey T. Dairiki. A lagrangian float. *Journal of Atmospheric and Oceanic Technology*, 13:1230 – 1246, 1996.

[Davis *et al.*, 1992] R. E. Davis, D.C. Webb, L.A. Regier, and J. Dufour. The autonomous lagrangian circulation explorer (alace). *Journal of Atmospheric Ocean Technology*, 9:264–285, 1992.

[Davis, 1991] Russ E. Davis. Observing the general circulation with floats. *Deep-Sea Research*, 38(Suppl. 1):531–571, 1991.

[Garau *et al.*, 2005] B. Garau, A. Alvarez, and G. Oliver. Path planning of autonomous underwater vehicles in current fields with complex spatial variability: an A* approach. In *Robotics and Automation, 2005. ICRA 2005. Proceedings of the 2005 IEEE International Conference on*, pages 194 – 198, april 2005.

[Hydroid, LLC, 2008] Hydroid, LLC. Remus 600. `http://www.hydroidinc.com/remus600.html`, 2008. viewed May 2008.

[King, 2004] I.P. King. *Update Documentation: RMA2 - A two-dimentional finite element model for flow in estuaries and streams*. Resource Modelling Associates, Sydney, Australia, 2004.

[Kruger *et al.*, 2007] D. Kruger, R. Stolkin, A. Blum, and J. Briganti. Optimal auv path planning for extended missions in complex, fast-flowing estuarine environments. In *Robotics and Automation, 2007 IEEE International Conference on*, pages 4265 –4270, april 2007.

[Manley and Wilcox, 2010] Justin Manley and Scott Wilcox. The wave glider, a persistent platform for ocean science. In *Proceedings of the MTS/IEEE OCEANS*, Sydney, Australia, May 2010.

[McGilvray and Roman, 2010] B. McGilvray and Chris Roman. Control system performance and efficiency for a mid-depth lagrangian profiling float. In *MTS/IEEE OCEANS 2010*, Sydney, Australia, May 2010.

[Morgansen *et al.*, 2007] Kristi A. Morgansen, B. I. Triplett, and D. J. Klein. Geometric methods for modeling and control of free-swimming fin-actuated underwater vehicles. *IEEE Transactions on Robotics*, 23(6):1184–1199, December 2007.

[Petres *et al.*, 2007] C. Petres, Y. Pailhas, P. Patron, Y. Petillot, J. Evans, and D. Lane. Path planning for autonomous underwater vehicles. *IEEE Transactions on Robotics*, 23(2):331–341, 2007.

[Roemmich *et al.*, 2004] Dean Roemmich, Stephen Riser, Russ Davis, and Yves Desaubies. Autonomous profiling floats: Workhorse for broad-scale ocean observations. *Marine Technology Society Journal*, 38:21–29, 2004.

[Rossby *et al.*, 1985] H.T. Rossby, E.R. Levine, and D.N. Connors. The isopycnal swallow float–a simple device for tracking water parcels in the ocean. *Progress In Oceanography*, 14:511 – 525, 1985.

[Schwithal and Roman, 2009] Alex Schwithal and Chris Roman. Development of a new lagrangian float for studying coastal marine ecosystems. In *MTS/IEEE OCEANS 2009*, Bremen Germany, 2009.

[Shchepetkin and McWilliams, 1998] A.F. Shchepetkin and J.C. McWilliams. Quasi-monotone advection schemes based on explicit locally adaptive dissipation. *Monthly Weather Review*, 126:1541–1580, 1998.

[Shchepetkin and McWilliams, 2005] Alexander F. Shchepetkin and James C. McWilliams. The regional oceanic modeling system (ROMS): a split-explicit, free-surface, topography-following-coordinate oceanic model. *Ocean Modelling*, 9:347–404, 2005.

[Smith *et al.*, 2010] Ryan N. Smith, Yi Chao, Peggy P. Li, David A. Caron, Burton H. Jones, and Gaurav S. Sukhatme. Planning and implementing trajectories for autonomous underwater vehicles to track evolving ocean processes based on predictions from a regional ocean model. *International Journal of Robotics Research*, 29(12):1475–1497, October 2010.

[Smith *et al.*, 2011] Ryan N. Smith, Mac Schwager, Stephen L. Smith, Burton H. Jones, Daniela Rus, and Gaurav S. Sukhatme. Persistent ocean monitoring with underwater gliders: Adapting sampling resolution. *Journal of Field Robotics*, 28(5):714 – 741, September/October 2011.

[Sussmann and Jurdjevic, 1972] H.J. Sussmann and V. Jurdjevic. Controllability of nonlinear systems. *Journal of Differential Equations*, 12:95–116, 1972.

[Sussmann, 1978] H.J. Sussmann. A sufficient condition for local controllability. *SIAM Journal on Control and Optimization*, 16(5):790–802, 1978.

[Webb Research Corporation, 2008] Webb Research Corporation. `http://www.webbresearch.com/slocum.htm`, 2008. viewed March 2011.

[Witt and Dunbabin, 2008] Jonas Witt and Matthew Dunbabin. Go with the flow: Optimal path planning in coastal environments. In J. Kim and R. Mahony, editors, *Proceedings of the 2008 Australasian Conference on Robotics & Automation (ACRA 2008)*, Canberra, ACT, 2008. ISBN: 9780646506432.